



A generalized exponential relationship between the surface-enhanced Raman scattering (SERS) efficiency of gold/silver nanoisland arrangements and their non-dimensional interparticle distance/particle diameter ratio

P. Pal^a, A. Bonyár^b, M. Veres^c, L. Himics^c, L. Balázs^a, L. Juhász^d, I. Csarnovics^{a,*}

^a Department of Experimental Physics, University of Debrecen, Debrecen, Hungary

^b Department of Electronics Technology, Budapest University of Technology and Economics, Budapest, Hungary

^c Institute for Solid State Physics and Optics, Wigner Research Centre for Physics, Budapest, Hungary

^d Department of Solid State Physics, University of Debrecen, Debrecen, Hungary

ARTICLE INFO

Article history:

Received 19 April 2020

Received in revised form 27 May 2020

Accepted 23 July 2020

Available online 25 July 2020

Keywords:

Gold and silver nanoislands
Surface-enhanced Raman scattering
Plasmonics
Photonic devices
Sensors

ABSTRACT

The optimization of the geometrical properties of gold/silver nanoparticle arrangements to maximize their surface-enhanced Raman scattering (SERS) efficiency is studied in this work. For this purpose, the metallic nanostructures were created by thermally annealing gold and silver thin film layers deposited onto glass substrates. The SERS capabilities of the samples were evaluated by measuring an analyte solution of benzophenone with three different excitation laser wavelengths. Systematic investigations were carried out on different gold and silver nanoisland samples to determine how the SERS enhancement depends on the geometrical (particle diameter, interparticle distance) and optical parameters (plasmon wavelength) of the nanostructures, as well as on the wavelength of laser excitation. The importance of matching the excitation wavelength with the resonant plasmon absorbance properties of the surface was proved. However, it was also shown that the optimization of the geometrical properties of the nanoisland arrangements dominates over the selection of the excitation wavelength. A generalized exponential relationship between the SERS enhancement and the non-dimensional interparticle distance/particle diameter ratio was established. Optimal technological parameters for the fabrication of gold/silver nanoisland SERS substrates were proposed.

© 2020 The Authors. Published by Elsevier B.V. This is an open access article under the CC BY-NC-ND license (<http://creativecommons.org/licenses/by-nc-nd/4.0/>).

1. Introduction

Raman spectroscopy is an efficient vibrational spectroscopic technique that allows the analysis of the structure and composition of materials in solid, liquid, or gas state [1]. The disadvantage is that Raman scattering has low scattering efficiency. Surface-enhanced Raman spectroscopy (SERS) is used for decades to improve the process sensitivity [2]. The SERS phenomenon was first observed in 1974 by Fleischmann et al. [3], who observed unexpectedly large Raman signals when studying pyridine adsorbed on a roughened silver electrode [4].

The magnification of Raman signals by several orders of magnitude is made possible by the nanostructured or roughened metal surface [5]. Several studies have addressed the SERS enhancement mechanism. Nowadays, it is accepted that two major factors contribute to the enhancement of Raman signals: electromagnetic [6] and chemical [7,8], from which the electromagnetic mechanism is considered to be the key one [6,9]. SERS incorporates the essential benefits of Raman spectroscopy such as fingerprint identification of molecules, non-destructive analysis, minimal sample preparation; analysis of biological samples; the possibility of carrying out field analysis using portable devices [8], all with high sensitivity, which in some cases even allows the detection of a single molecule [4,10].

Silver and gold nanostructures are the most widely used materials in SERS substrates due to their surface plasmon resonance (LSPR) properties, which cover a wide wavelength range in the visible and near-infrared regions where most Raman measurements are made [1,11]. Several methods have been developed for the fabrication of these substrates, which follow one of two gen-

* Corresponding author at: Department of Experimental Physics, Institute of Physics, Faculty of Science and Technology, University of Debrecen, 4026 Debrecen Bem sq 18/a, Hungary.

E-mail address: csarnovics.istvan@science.unideb.hu (I. Csarnovics).

eral strategies: top-down and bottom-up [10,12]. The top-down strategy is based on micro- and nanofabrication techniques (electron beam lithography [13], atomic layer deposition [14], focused ion beam [15] nanosphere lithography [16]). On the contrary, the bottom-up strategy relies on chemical synthesis and assembly that offers the opportunity to prepare cost-effective SERS substrates. The morphology of chemically synthesized nanostructures includes nanospheres [17–19], nanocubes [20], nano triangles [21], nanorods [22], and nucleus nanostructures [23,24]. Each technology is capable of controlling the parameters (dimensions, shape) of the nanoparticles. This is important because the enhancement of the SERS effect is influenced by these parameters and other factors as well [24,25].

Nowadays, research focuses on the structural properties of SERS substrates [26,27] and the development and fabrication of substrates with optimal enhancement properties [4]. The SERS enhancement factor (SERS EF) of a substrate depends on several factors, such as the geometrical properties of the nanoparticles (size, shape, interparticle distance, and general arrangement) or the wavelength of the excitation source [28]. These factors are intertwined in a nontrivial way, forming a complex system, which is essential to be optimized for the best SERS performance.

The effect of nanoparticle size on the SERS performance was previously studied [29–32] with mixed conclusions. It was shown that the highest SERS EF could be reached with spherical gold and silver nanoparticles with a diameter of 50 nm [29,31], while others reported a broader range of optimal particle sizes between 30–100 nm for the improvement of SERS [30,32]. Generally, when the particles are too small, both the actual conductivity and the scattering properties are reduced, which expectedly reduces the SERS efficiency [30]. As the particle size increases, the SERS effect increases since they act as larger scattering centers. However, in these papers, there was no study concerning the interparticle distance.

Besides, other works studied this parameter, as interparticle distance also affects the SERS enhancement. In previous works, a relationship between the interparticle distance and the SERS enhancement was demonstrated [33,34]. The closer the particles are to each other, the higher the specific surface coverage of their active surfaces is, and the surface density of hot-spots (number of areas with increased near field intensities due to coupled plasmons between the particles) is also higher, which altogether results in an improved SERS efficiency as it was shown in our previous work [35]. At very short distances (e.g., less than 1 nm), quantum mechanical phenomena play a role that limits the possible achievable field strengths [36]. Most papers only study the influence of interparticle distance and do not take into account the effect of the nanostructures' size, except for a few [35,37–39]. It could be concluded that several past works investigated the effect of these parameters independently; their complex relationship is not yet fully described.

The shape of the nanoparticles can also be a factor, its effect on the SERS enhancement was investigated by others [40–42]. According to these, anisotropic metallic nanoparticles with complex shapes (e.g., hexagonal, triangular, cubical, star shape), could be beneficial due to the more intense near-fields at the sharp edges. However, the complicated synthesis of some of these particles and their subsequent surface chemistry are the main drawback of their current application.

Another general consideration is that the wavelength of the excitation source should match the plasmonic properties (LSPR excitation range) of the substrate as close as possible. The LSPR absorbance wavelength shifts to red with larger nanoparticle size and smaller interparticle distance (due to the plasmonic coupling) [43,44]. If the excitation wavelength is far from the plasmon excitation of the substrate, the SERS enhancement can

be reduced [25,35]. The fine-tuning of all these parameters is the key to optimize the SERS substrate properties to maximize their enhancement factor [45].

In this study, SERS substrates based on gold and silver nanoislands were prepared on glass substrates with different technological parameters. The effect of material type, particle size, interparticle distance (which altogether determine the plasmonic properties of the substrates) and the excitation wavelength on the SERS enhancement was studied in detail. The complex relationship between the size of the nanoparticles, the interparticle distance, and the enhancement factor is studied and demonstrated comprehensively. For this purpose, a benzene derivative (benzophenone) dissolved in isopropyl alcohol was used as a target material, for its characteristic and identifiable phenol related peaks. Regarding the application of SERS for the detection of other materials systems, some recent reviews can be recommended [46,47].

2. Materials and methods

2.1. Preparation of SERS substrates

The substrates for the SERS active nanoparticles were cut from microscope slides with a handheld glass cutter to form glass plates. They were cleaned in an EMMI-20HC ultrasonic bath in 96% ethanol and then wiped dry with a sterile paper. The amount of material to be evaporated was measured on a Sartorius Micro M3p semi-micro analytical balance. The thin metallic films with controlled thicknesses were prepared by thermal evaporation. The layer thickness was measured by using an Ambios XP-1 profilometer. The thicknesses of the created gold layers were 9 and 12 nm, while for the silver layer 15 and 25 nm. Samples were then heat-treated in a quartz glass tube placed in an oven filled with Ar:H precursor gas. The heat treatment (solid-state dewetting) took place at different temperatures (350 °C, 450 °C, and 550 °C) for different periods (15, 30, 60 and 120 min), resulting in a variety of geometrical parameters (e.g., particle diameter, interparticle distance). During the treatment, the high temperature induces diffusion on the surface of the substrate, causing the thin film first to burst, then to form nanoscale islands.

2.2. Characterization of SERS substrates

The freshly prepared metallic nanoislands were examined by using a scanning electron microscope (SEM) and then an optical spectrophotometer. SEM images were recorded with a Hitachi S4300-CFE instrument. Multiple locations and magnifications were taken on each sample. The images were evaluated by using the National Instruments Vision Assistant software package, which determined the mean nanoisland diameter (defined as the equivalent diameter of a circle having the same projected area as the nanoisland), measurement uncertainty, and diameter distribution.

To further evaluate the diameter distribution, we used the OriginPro 9 software and a custom-written Matlab script to determine the average interparticle distance and its standard deviation. The measurement uncertainty of the diameter of the produced nanostructures and the interparticle distance was 10–15 %, depending on the sample. The next step was to investigate the plasmon wavelength of the created metallic nanostructures. Measurements were made with an OceanOptics Red Tide USB650 optical fiber spectrophotometer. The optical transmittance of the samples was measured in air.

Figs. 1 and 2 illustrates SEM images (with an acceleration voltage of 5 kV and magnification of $\times 20\,000$ or $\times 30\,000$) of gold and silver nanoislands and their transmittance spectra. The diameter, interparticle distance, and plasmon wavelengths could be controlled by

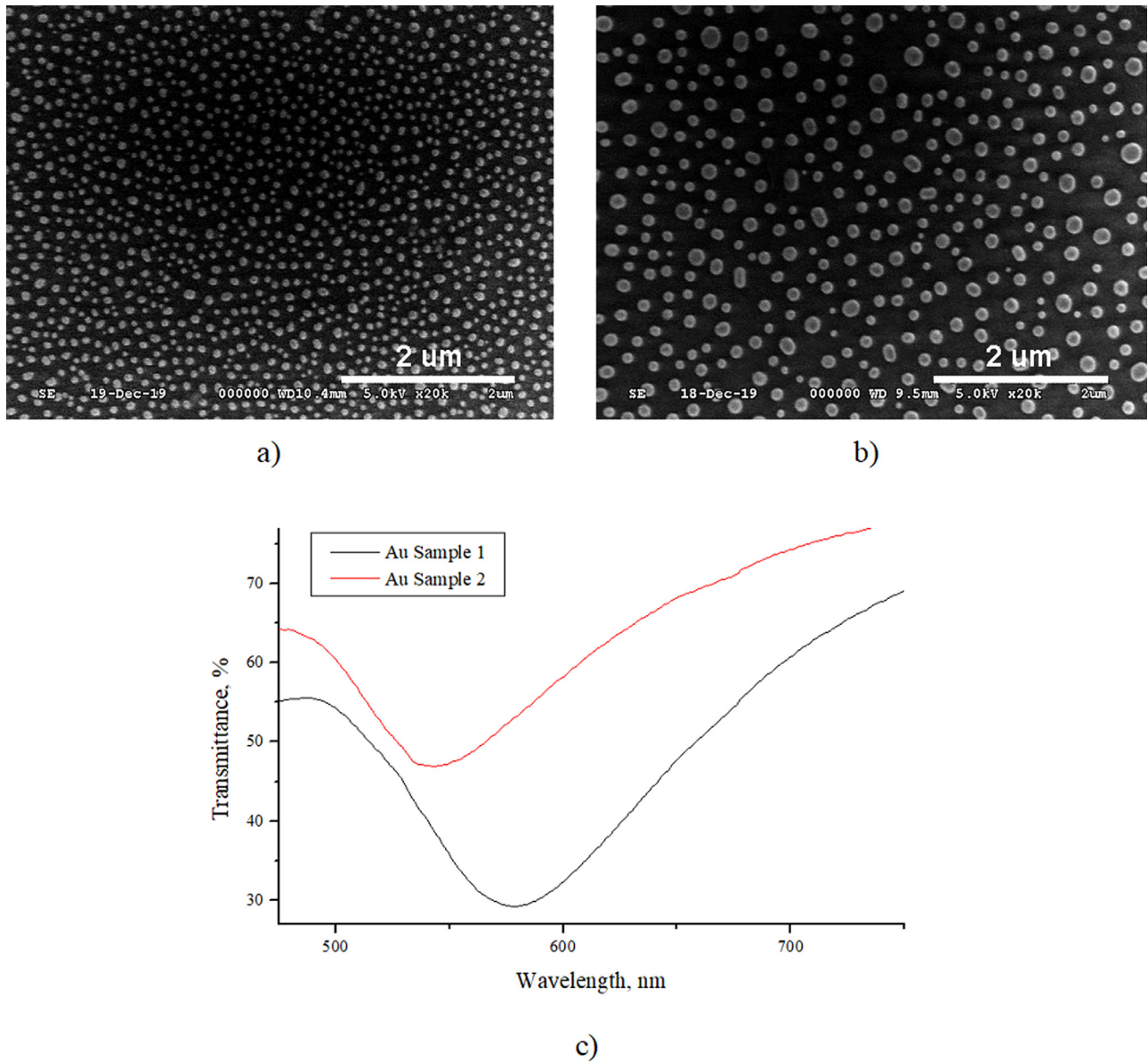


Fig. 1. Illustration of the prepared gold nanoislands: a) SEM image of gold sample 1; b) SEM image of gold sample 2; c) The corresponding optical transmittance spectra of the samples. The technological parameters are given in Table 1. The magnification of SEM images was $\times 20\,000$.

Table 1

Parameters of the two different gold samples.

	Au Sample 1	Au Sample 2
Initial layer thickness	9 nm	12 nm
Annealing temperature	550 °C	550 °C
Annealing time	15 min	15 min

Table 2

Parameters of the two different silver samples.

	Ag Sample 1	Ag Sample 2
Initial layer thickness	15 nm	25 nm
Annealing temperature	350 °C	350 °C
Annealing time	60 min	60 min

the initial thickness while keeping the annealing temperature and time fixed. Fig. 1 and 2 illustrate two different gold/silver samples with the fabrication parameters given in Tables 1 and 2, respectively. These figures show how the initial layer thickness affects

the diameter of the formed nanoislands and the interparticle distance at the same annealing temperature and time. By starting from a thicker layer, larger nanoislands are formed farther apart, while a thinner film produces smaller nanoislands that are closer together. Also, the different gold and silver patterns clearly show how the transmittance of the sample varies with diameter, affected by the initial layer thickness.

2.3. Sample preparation for SERS measurements

The analyte solution used for the Raman measurements was 50 mM benzophenone, dissolved in isopropyl alcohol, and all SERS measurements were performed with a solution taken from the same batch. During the preparation, special care was given to dissolve all the benzophenone crystals and to homogenize the solution.

Spin coater was used to place the benzophenone solution on the SERS substrates, which allows creating a uniform thin layer of the analyte. The substrates were placed in the center of the

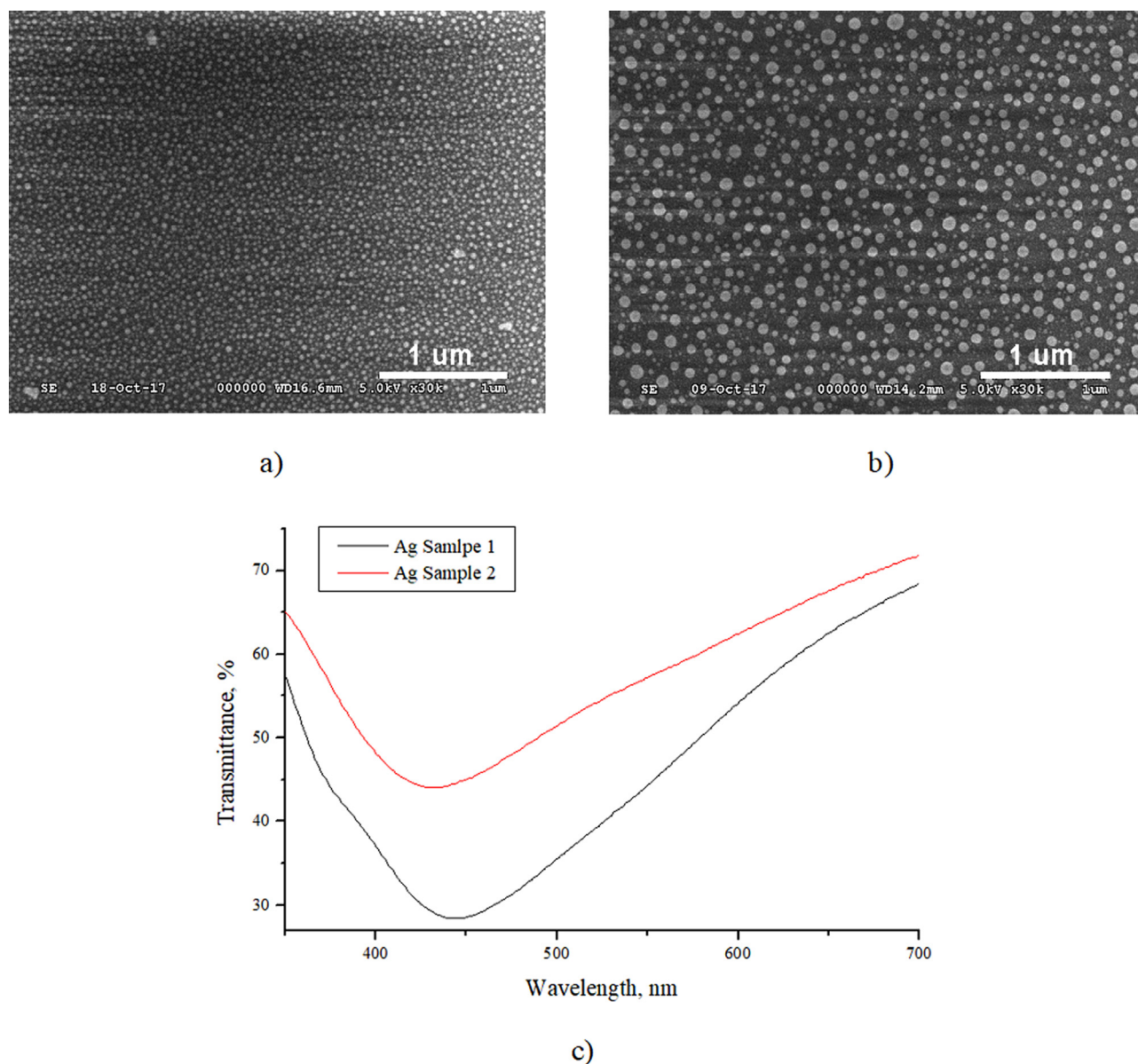


Fig. 2. Illustration of the prepared silver nanoislands: a) SEM image of silver sample 1; b) SEM image of silver sample 2; c) The corresponding optical transmittance spectra of the samples. The technological parameters are given in Table 2. The magnification of SEM images was $\times 30\,000$.

device, which was fixed with double-sided adhesive. Then, using a micropipette, 20 μL of the sample solution was dropped into the center of the active surface, and the spin coater was started and rotated at 1000 rpm for 1 min. The centrifugal force occurring during high-speed rotation uniformly distributes the solution on the substrate surface.

2.4. SERS measurements

A Renishaw inVia, a Renishaw 1000B, and a Horiba LabRam Raman spectrometer were used for Raman measurements on the samples. During the work, 488, 532, and 633 nm lasers were used as excitation sources, and the measurement time for each sample was 10 s. The excitation beam was focused onto the sample surface with a 50x lens. Raman measurements were performed in several points on the substrate surface (5–7 points), and the measurement has been repeated in the point where the SERS enhancement proved to be the best. For the reference Raman spectrum, the analyte was

placed on a bare glass slide under the same conditions and in the same amount.

The characteristic spectra of benzophenone were obtained in our measurements on a pure glass substrate and metallic nanoparticles as well. The main bands of benzophenone can be observed on both with different intensities (see Fig. 3). Based on these, the SERS enhancement was calculated from the intensity of the 1596 cm^{-1} peak, which corresponds to the vibration of the C–C bonds of the phenyl ring [48].

In this work, we calculated the SERS enhancement based on the enhancement factor (EF) [9], which can be defined as Eq. (1):

$$EF = \frac{I_{\text{SERS}}/N_{\text{SERS}}}{I_{\text{RS}}/N_{\text{RS}}} \quad (1)$$

In this approach, I_{RS} is the Raman signal under non-SERS conditions (e.g., on the surface of the reference sample). Under the same experimental conditions and the same preparation conditions, the SERS signal measured on the SERS substrate will have the intensity of I_{SERS} [9,30]. At the same time, the N_{RS} – is the aver-

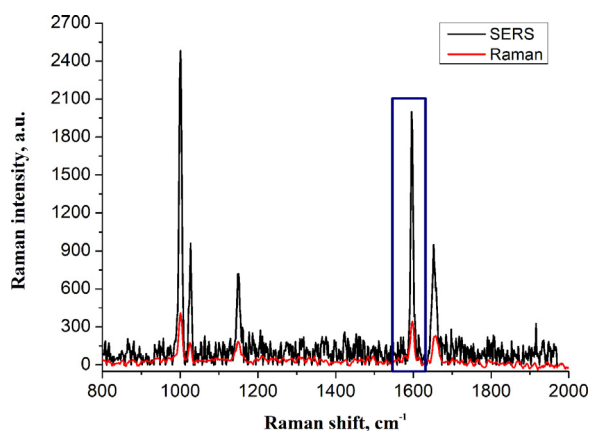


Fig. 3. The measured Raman and SERS spectra of the benzophenone.

age number of molecules in the scattering volume for the Raman (non-SERS) measurement, and N_{SERS} – is the average number of adsorbed molecules in the scattering volume for the SERS experiments. This EF calculation approach ignores the fact that SERS is a surface-sensitive phenomenon: only surface-adsorbed molecules contribute to the highest EM enhancement, and the signal contribution decays exponentially with increasing distance to the surface. Since in our experiments, the sample was present only in the form of a thin spin-coated layer (for both SERS and reference measurements) we assumed that $N_{\text{SERS}} \cong N_{\text{RS}}$, thus EF can be simplified as the ratio of the measured intensities.

3. Results and discussion

3.1. Gold substrates

For both gold and silver nanoislands, measurements were made with three lasers of different wavelengths. Before that, their optical parameters, diameter, and interparticle distance were measured, and the EF was evaluated for each excitation wavelength.

As mentioned in the introduction, the relationship between the plasmon wavelength of the substrate and the excitation wavelength affects the SERS enhancement. The three different excitation wavelengths in our study are meant to probe this relationship. The plasmon resonance of nanoislands can be effectively tuned with the particle diameter, structure, and interparticle distance [33,38,39].

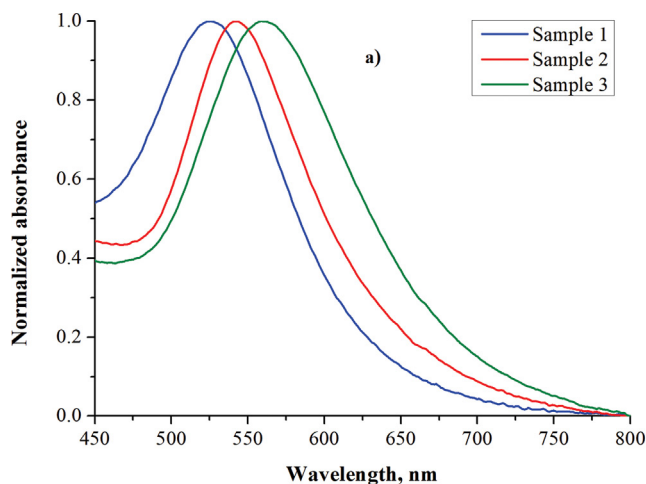


Fig. 4. a) Normalized absorbance spectra illustrating the effect of different gold nanoisland diameters on the plasmonic absorbance of the substrates (average diameters: #1: 50 nm, #2: 54 nm, #3: 75 nm); b) Dependence of the enhancement factor on the excitation wavelength in the function of the normalized absorbance at that wavelength. For this, the normalized absorbance of the samples (as in Fig. 4a) were evaluated at the excitation laser's wavelength.

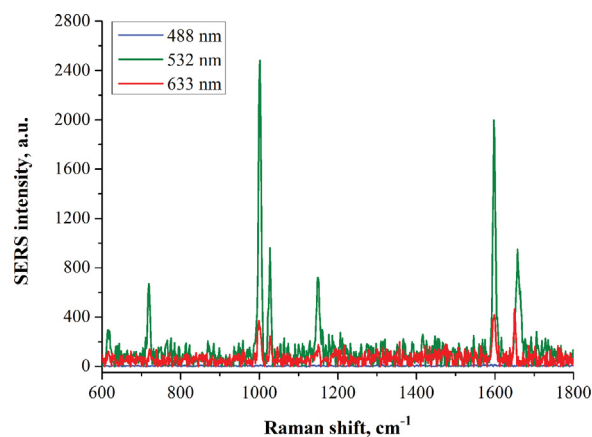
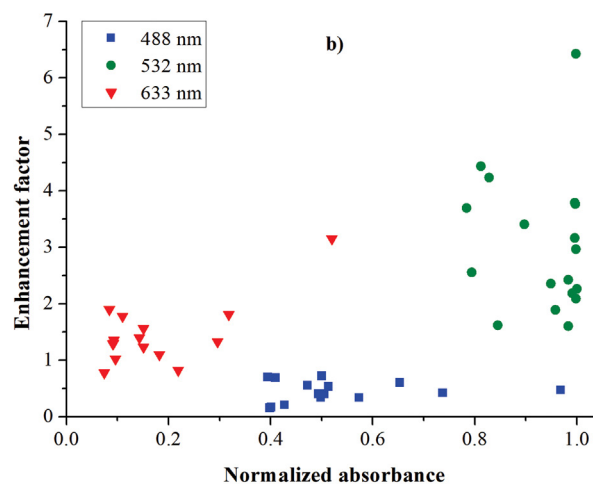


Fig. 5. Surface-enhanced Raman spectra of benzophenone measured on a gold nanoisland substrate with three different excitation wavelengths.

Fig. 4a illustrates the effect of the nanoisland diameter on the plasmon wavelength. The measured diameter, interparticle distance and plasmon wavelength of the three nanoisland arrangements shown in the figure are the following: sample 1: 50 nm, 45 nm, 514 nm, sample 2: 54 nm, 46 nm, 527 nm, sample 3: 59 nm, 37 nm, 561 nm, respectively. It can be seen that by increasing the diameter of the gold nanoislands, the position of the plasmon peak is shifting to higher wavelengths. The relationship between the plasmon absorbance properties and the excitation wavelengths can be studied based on Fig. 4b. Since the plasmon resonance of the gold nanoislands is in the 500–600 nm range, it can be expected that the laser with 532 nm excitation wavelength will yield the highest SERS enhancement. Fig. 4b partially confirm this, since, in general, the 532 nm excitation resulted in the highest average EF. Fig. 5 presents sample Surface-enhanced Raman spectra measured with the three different excitation sources, which also illustrate that the highest enhancement was obtained by using 532 nm excitation. It should be noted that the Raman scattering will be non-resonant for all these excitation wavelengths. The analysis of the absorption spectrum of benzophenone [49] shows that the absorption bands of the compound are in the UV region, well below our lowest laser wavelength of 488 nm.

However, there are some peculiarities worth mentioning. In Fig. 4b, the presented data are given as a function of the normalized absorbance measured at the given excitation wavelength. A higher



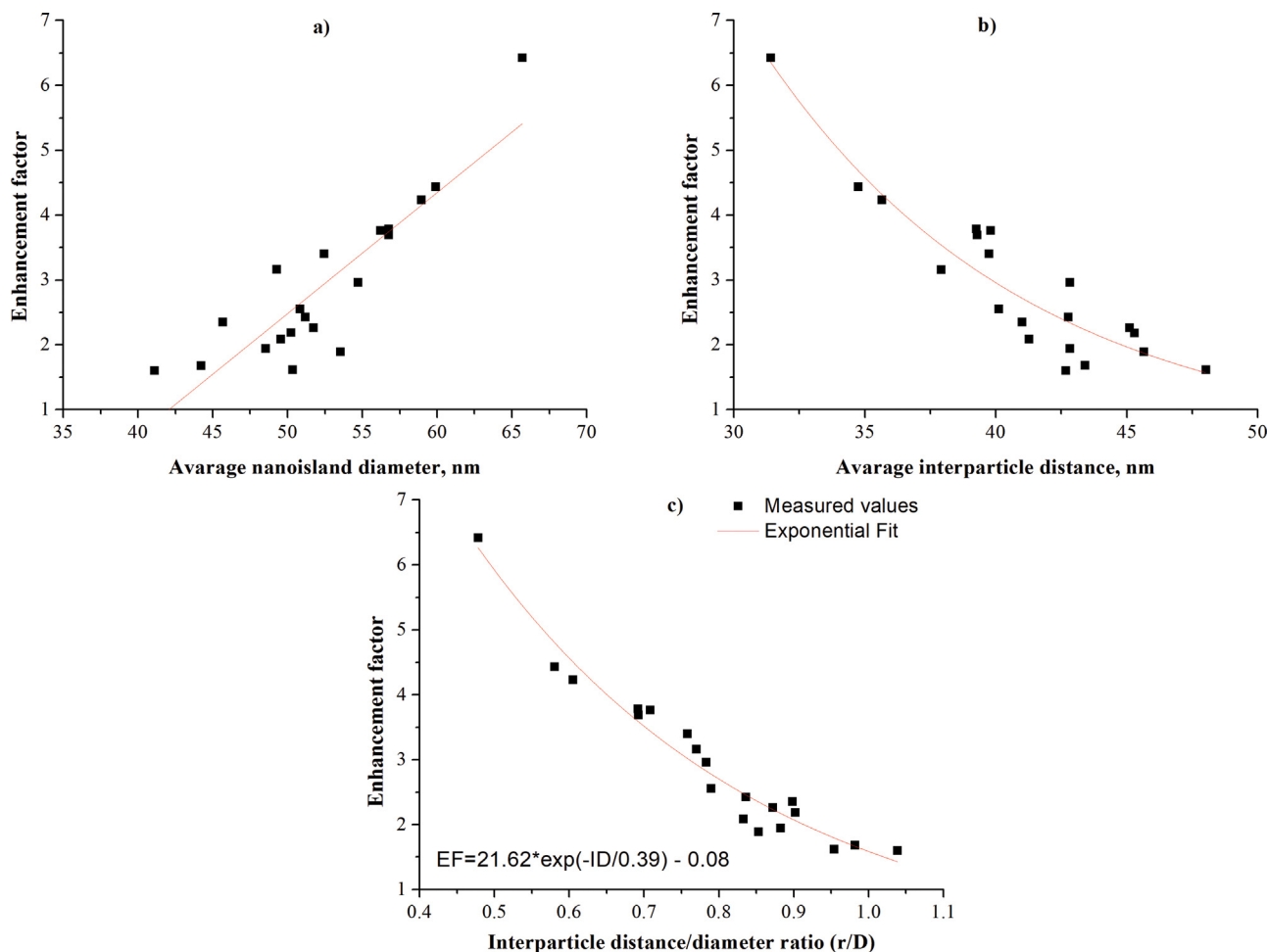


Fig. 6. Enhancement factors obtained for 532 nm excitation, in the function of a) the average gold nanoisland diameter (D); b) the average interparticle distance (r); and c) the interparticle distance/nanoisland diameter ratio (r/D).

normalized absorbance means that the nanoparticle arrangement has a stronger plasmonic resonance at the given wavelength. The fact that the EF does not correlate directly with the normalized absorbance indicates that the excitation wavelength is important not only because of its relation to plasmon excitation. E.g., in some of the cases, a 633 nm excitation with small normalized absorbance (around 0.1, in other words far from the plasmon resonance peak) resulted in better enhancement than the 532 nm excitation with high normalized absorbance (around 1, e.g., in the plasmon resonance peak). Also, the 488 nm excitation resulted in the smallest average EF regardless of the normalized absorbance at this wavelength. These observations indicate that other factors determine or influence the effect of excitation wavelength on the SERS EF besides its relation to the plasmonic properties of the substrate.

To evaluate the effect of the geometrical parameters on the measured SERS enhancement factors in more detail, the resulting EFs obtained with the 532 nm laser excitation were plotted as a function of both the average nanoisland diameter (Fig. 6a) and the average interparticle distance (Fig. 6b). As expected – according to the discussions in the introduction – the measured EF shows a strong positive linear correlation with the particle size and also decays exponentially with increasing interparticle distance. The variation of the data decreases significantly when the obtained EFs are plotted as a function of the interparticle distance/nanoisland diameter ratio (r/D). The enhancement factor shows a clear exponential relationship with this non-dimensional parameter (equation given in Fig. 6c, in which the ID is the interpar-

ticle distance/nanoisland diameter ratio), which makes the design and optimization of the SERS substrates simpler.

Based on the results, the highest SERS enhancement (~ 6.5) was achieved with gold nanoislands prepared with the following fabrication parameters: initial layer thickness: 9 nm, annealing temperature: 500 °C, annealing time: 15 min. The SERS substrate fabricated with these conditions has the following parameters: plasmon wavelength peak: 528 nm, particle diameter: 58 nm, interparticle distance: 30 nm.

3.2. Silver substrates

The silver-based nanoisland SERS substrates were investigated with the same methodology. Fig. 7a shows the three typical spectra with the following geometrical and plasmonic properties (diameter, interparticle distance, and plasmon wavelength): sample 1: 34 nm, 41 nm, 422 nm, sample 2: 37 nm, 36 nm, 436 nm, sample 3: 39 nm, 31 nm, 445 nm. For the silver nanoisland samples, the plasmon absorbance peaks are between 400–460 nm, thus, as expected, the highest average enhancement factors were achieved with the 488 nm laser excitation (see Fig. 7b). This is also confirmed by the sample Surface-enhanced Raman spectra presented in Fig. 8. However, similarly to what we saw in the case of the gold nanoislands, the measured EF does not correlate clearly with the normalized absorbance, regardless of the excitation wavelength (Fig. 7b).

As in the case of gold nanoislands, the effect of the geometrical parameters was studied in detail. The charts of Fig. 9 show

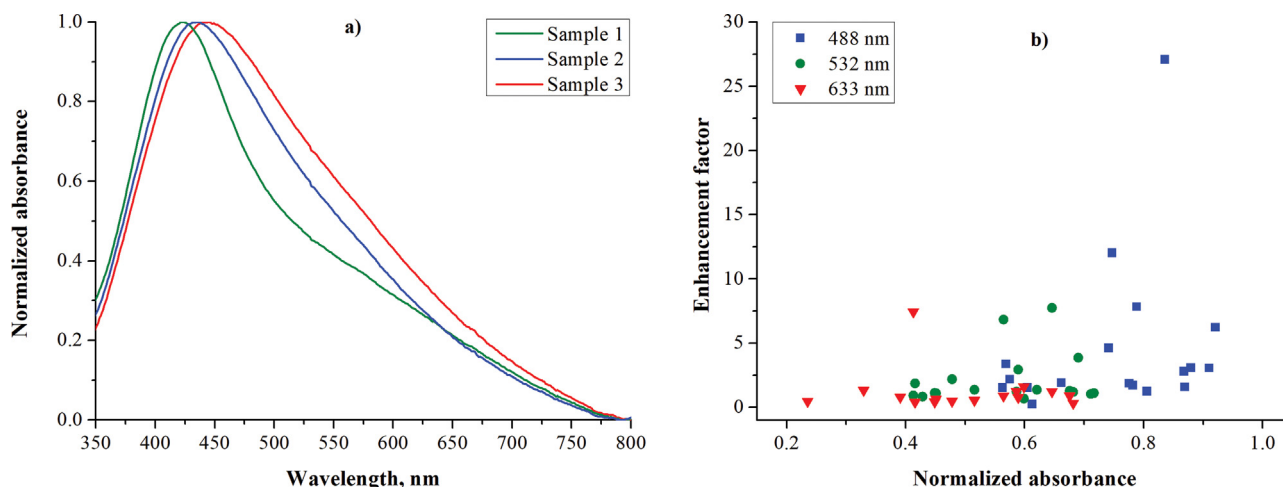


Fig. 7. a) Normalized absorbance spectra illustrating the effect of different silver nanosland diameters on the plasmonic absorbance of the substrates (average diameters: #1: 34 nm, #2: 37 nm, #3: 39 nm); b) Dependence of the enhancement factor on the excitation wavelength in the function of the normalized absorbance at that wavelength. For this, the normalized absorbance of the samples (as in Fig. 7a) were evaluated at the excitation laser's wavelength.

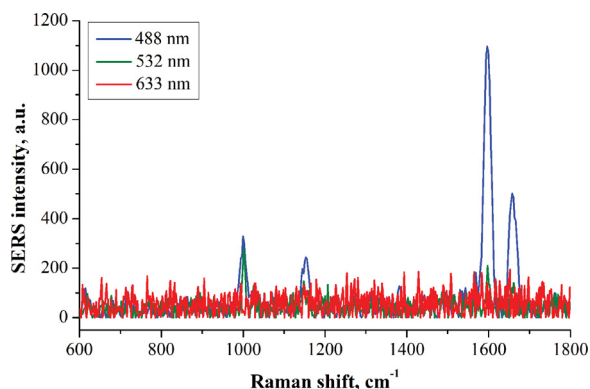


Fig. 8. Surface-enhanced Raman spectra of benzophenone measured on a silver nanosland substrate with three different excitation wavelengths.

the same linear and exponential tendencies between the measured EF and the nanosland diameter and interparticle distance, respectively (for the data obtained with the 488 nm excitation). The EF also shows a clear exponential relationship with the non-dimensional (r/D) parameter (equation in Fig. 9c, where ID is the interparticle distance/nanosland diameter ratio). It has to be noted that silver nanoslands show a higher respective SERS enhancement in the function of r/D (by comparing the equations in Figs. 6c and 9 c).

The highest SERS enhancement (~ 27) was achieved with silver nanoslands prepared with the following fabrication parameters: initial layer thickness: 25 nm, annealing temperature: 350 °C, annealing time: 60 min. The SERS substrate fabricated with these conditions has the following parameters: plasmon wavelength peak: 438 nm, particle diameter: 61 nm, interparticle distance: 22 nm.

4. Conclusions

By comparing the results obtained on the gold and silver nanosland arrangements, we can draw the following conclusions:

1) The highest average and maximum obtained SERS analytical enhancement factors were achieved with the 532 nm laser irradiation for gold nanoslands and with the 488 nm excitation for silver nanoslands. This proves that the relationship between the excitation wavelength and the plasmon absorbance properties of the

surface is important and should be considered when selecting a SERS substrate.

2) Our findings partially contradict the fact that for both of the cases, the obtained EFs did not show a clear correlation with the normalized absorbance peaks considering all investigated excitation wavelengths. This suggests that other factors – such as the geometrical properties of the nanosland arrangements – dominate over the excitation wavelength to a reasonable extent.

3) The SERS EF showed a positive linear correlation with the nanoparticle size and a negative exponential relation with the interparticle distance for both types of nanomaterials. This can be attributed to the higher scattering efficiency (bigger particle size) and the higher density of near-field hot spots on the surface in the case of tightly packed particles.

4) A precise exponential relationship could be established between the measured EF and the non-dimensional r/D parameter, which is the ratio of the interparticle distance and the particle diameter, for both material types.

5) Silver nanoslands (measured at 488 nm) showed a steeper exponential increase in the EF with decreasing r/D compared to the gold nanoslands (measured at 532 nm excitation).

6) These results suggest that larger and closer packed metallic nanostructures will result in better SERS enhancement. In the case of gold, this can be achieved with a thinner starting layer (6 nm), lower annealing temperature (450 °C) and longer annealing time (30–60 min), or a thicker layer (9 nm), higher temperature (500 °C), and shorter time (15 min). In the case of silver, larger and denser nanoslands were achieved with a thicker starting layer (25 nm), low annealing temperature (350 °C), and longer time (60–120 min).

7) These sets of technological parameters result in smaller average r/D parameters for the silver nanoslands and thus higher SERS enhancement factors, compared to the gold nanoslands.

Declaration of Competing Interest

Please check the following as appropriate:

- All authors have participated in (a) conception and design, or analysis and interpretation of the data; (b) drafting the article or revising it critically for important intellectual content; and (c) approval of the final version.
- This manuscript has not been submitted to, nor is under review at, another journal or other publishing venue.

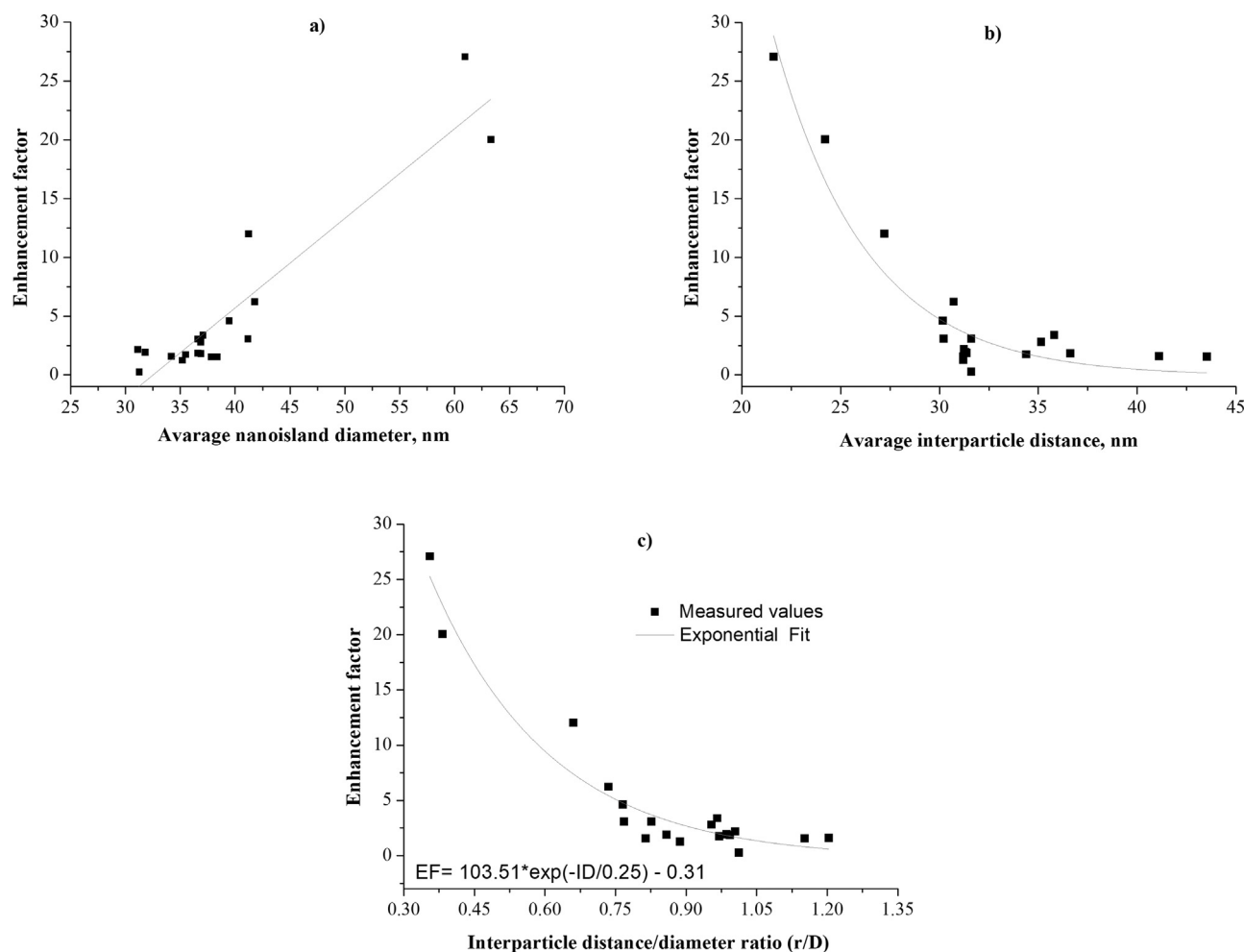


Fig. 9. Enhancement factors obtained for 488 nm excitation, in the function of a) the average silver nanoisland diameter (D); b) the average interparticle distance (r); and c) the interparticle distance/nanoisland diameter ratio (r/D).

- The authors have no affiliation with any organization with a direct or indirect financial interest in the subject matter discussed in the manuscript
- The following authors have affiliations with organizations with direct or indirect financial interest in the subject matter discussed in the manuscript:

Declaration of Competing Interest

The authors report no declarations of interest.

Acknowledgments

This work was financially supported by the grant GINOP-2.3.2-15-2016-00041. The project is co-financed by the European Union and the European Regional Development Fund. This work was supported by the VEKOP-2.3.2-16-2016-00011 grant, which is co-financed by the European Union and European Social Fund. The research reported in this paper was partially supported by the Higher Education Excellence Program of the Ministry of Human Capacities in the frame of Nanotechnology and Materials Science (BME FIKP-NAT) and also Biotechnology (BME-FIKP-BIO) research areas of Budapest University of Technology and Economics. Istvan Csarnovics is grateful for the support of the János Bolyai Research Scholarship of the Hungarian Academy of Sciences. The support

through the New National Excellence Program of the Ministry of Human Capacities is acknowledged as well.

Appendix A. Supplementary data

Supplementary material related to this article can be found, in the online version, at doi:<https://doi.org/10.1016/j.sna.2020.112225>.

References

- [1] L.T. Hoang, H.V. Pham, M.T.T. Nguyen, Investigation of the factors influencing the surface-enhanced raman scattering activity of silver nanoparticles, *J. Electron. Mater.* (2019) 1–8, <http://dx.doi.org/10.1007/s11664-019-07870-8>.
- [2] C.L. Haynes, C.R. Yonzon, X. Zang, R.P. Van Duyne, Surface-enhanced Raman sensors: early history and the development of sensors for quantitative biowarfare agent and glucose detection, *J. Raman Spectrosc.* 36 (2005) 471–484, <http://dx.doi.org/10.1002/jrs.1376>.
- [3] M. Fleischmann, P.J. Hendra, A.J. McQuillan, Raman spectra of pyridine adsorbed at a silver electrode, *ChemR. Phys. Lett.* 26 (1974) 163–166, [http://dx.doi.org/10.1016/0009-2614\(74\)85388-1](http://dx.doi.org/10.1016/0009-2614(74)85388-1).
- [4] R. Pilot, R. Signorini, C. Durante, L. Orian, M. Bhamidipati, L. Fabris, A review on surface-enhanced raman scattering, *Biosensors.* 9 (2019) 1–100, <http://dx.doi.org/10.3390/bios9020057>.
- [5] J. Choi, J.-H. Kim, J.-W. Oh, J.-M. Nam, Surface-enhanced raman scattering-based detection of hazardous chemicals in various phases and matrices with plasmonic nanostructures, *Nanoscale.* 11 (2019) 20379–20391, <http://dx.doi.org/10.1039/c9nr07439b>.
- [6] S.-Y. Ding, E.-M. You, Z.-Q. Tian, M. Moskovits, Electromagnetic theories of surface-enhanced Raman spectroscopy, *Chem. Soc. Rev.* 46 (2017) 4042–4076, <http://dx.doi.org/10.1039/c7cs00238f>.

- [7] A. Otto, The “chemical” (electronic) contribution to surface-enhanced Raman scattering, *J. Raman Spectrosc.* 36 (2005) 497–509, <http://dx.doi.org/10.1002/jrs.1355>.
- [8] A. Otto, Charge transfer in first layer enhanced Raman scattering and surface resistance, *Q. Phys. Rev.* 3 (2017) 1–14.
- [9] H.K. Lee, Y.H. Lee, C.S.L. Koh, G.C. Phan-Quang, X. Han, C.L. Lay, X.Y. Ling, H.Y.F. Sim, Y.-C. Kao, Q. An, Designing surface-enhanced Raman scattering (SERS) platforms beyond hot-spot engineering: emerging opportunities in analyte manipulations and hybrid materials, *Chem. Soc. Rev.* 48 (2019) 731–756, <http://dx.doi.org/10.1039/c7cs00786h>.
- [10] H. Chu, S. Song, C. Li, D. Gibson, Surface enhanced Raman scattering substrates made by oblique angle deposition: methods and applications, *Coatings* 7 (2017) 1–23, <http://dx.doi.org/10.3390/coatings7020026>.
- [11] P.A. Mosier-Boss, Review of SERS substrates for chemical sensing, *Nanomaterials* 7 (2017) 142.
- [12] S.-Y. Ding, X.-M. Zhang, B. Ren, Z.-Q. Tian, Surface-enhanced Raman spectroscopy (SERS): general introduction, *Encyclopedia of Analytical Chemistry* (2014) 1–34, <http://dx.doi.org/10.1002/9780470027318.a9276>.
- [13] Z.-Q. Tian, B. Ren, Infrared and Raman spectroscopy in analysis of surfaces, *Encyclopedia of Analytical Chemistry* (2006) 1–40, <http://dx.doi.org/10.1002/9780470027318.a2516>.
- [14] J. Theiss, P. Pavaskar, P.M. Echternach, R.E. Muller, S.B. Cronin, Plasmonic nanoparticle arrays with nanometer separation for high-performance SERS substrates, *Nano Lett.* 10 (2010) 2749–2754, <http://dx.doi.org/10.1021/nl904170g>.
- [15] X.Y. Zhang, J. Zhao, A.V. Whitney, J.W. Elam, R.P. Van Duyne, Ultrastable substrates for surface enhanced Raman spectroscopy: Al₂O₃ overlayers fabricated by atomic layer deposition yield improved anthrax biomarker detection, *J. Am. Chem. Soc.* 128 (2006) 10304–10309, <http://dx.doi.org/10.1021/ja0638760>.
- [16] J.T. Bahns, A. Imre, V.K. Vlasko-Vlasov, J. Pearson, J.M. Hiller, L.H. Chen, U. Welp, Enhanced Raman scattering from focused surface plasmons, *Appl. Phys. Lett.* 91 (2007) 081104, <http://dx.doi.org/10.1063/1.2759985>.
- [17] J.N. Anker, W.P. Hall, O. Lyandres, N.C. Shah, J. Zhao, R.P. Van Duyne, Biosensing with plasmonic nanosensors, *Nat. Mater.* 7 (2008) 442–453, <http://dx.doi.org/10.1038/nmat2162>.
- [18] K.C. Grabar, R.G. Freeman, M.B. Hommer, M.J. Natan, Preparation and characterization of Au colloid monolayers, *Anal. Chem.* 67 (1995) 735–743, <http://dx.doi.org/10.1021/ac00100a008>.
- [19] A. Wei, B. Kim, B. Sadler, S.L. Tripp, Tunable surface-enhanced Raman scattering from large gold nanoparticle arrays, *Chemphyschem.* 12 (2001) 743–745, [doi:10.1002/1439-7641\(20011217\)2:12<743::aid-cphc743>3.0.co;2-1](http://dx.doi.org/10.1002/1439-7641(20011217)2:12<743::aid-cphc743>3.0.co;2-1).
- [20] P.Z. El-Khoury, E. Khon, Y. Gong, A.G. Joly, P. Abellan, J.E. Evans, N.D. Browning, D.Hu M. Zamkov, Electric field enhancement in a self-assembled 2D array of silver nanospheres, *J. Chem. Phys.* 141 (2014) 214308, <http://dx.doi.org/10.1063/1.4902905>.
- [21] H. Chen, Z.H. Sun, W.H. Ni, K.C. Woo, H.Q. Lin, L.D. Sun, C.H. Yan, J.F. Wang, Plasmon coupling in clusters composed of two-dimensionally ordered gold nanocubes, *Small* 5 (2009) 2111–2119, <http://dx.doi.org/10.1002/sml.200900256>.
- [22] M. Rycenga, C.M. Cobley, J. Zeng, W.Y. Li, C.H. Moran, Q. Zhang, D. Qin, Y.N. Xia, Controlling the synthesis and assembly of silver nanostructures for plasmonic applications, *Chem. Rev.* 111 (2011) 3669–3712, <http://dx.doi.org/10.1021/cr100275d>.
- [23] J. Kumar, K.G. Thomas, Surface-enhanced Raman spectroscopy: investigations at the nanorod edges and dimer junctions, *J. Phys. Chem. Lett.* 2 (2011) 610–615, <http://dx.doi.org/10.1021/jz2000613>.
- [24] L. Zhang, C. Guan, Y. Wang, J. Liao, Highly effective and uniform SERS substrates fabricated by etching multi-layered gold nanoparticle arrays, *Nanoscale* 8 (2016) 5928–5937, <http://dx.doi.org/10.1039/c6nr00502k>.
- [25] N.D. Israelsen, C. Hanson, E. Vargis, Nanoparticle properties and synthesis effects on surface-enhanced Raman scattering enhancement factor: an introduction, *The Scientific World Journal* (2015) 1–12, <http://dx.doi.org/10.1155/2015/124582>.
- [26] S.L. Kleinman, B. Sharma, M.G. Blaber, A.I. Henry, N. Valley, R.G. Freeman, M.J. Natan, G.C. Schatz, R.P. Van Duyne, Structure enhancement factor relationships in single gold nanoantennas by surface-enhanced Raman excitation spectroscopy, *J. Am. Chem. Soc.* 135 (2013) 301–308, <http://dx.doi.org/10.1021/ja309300d>.
- [27] E.C. Le Ru, J. Grand, N. Félidj, J. Aubard, G. Lévi, A. Hohenau, J.R. Krenn, E. Blackie, P.G. Etchegoin, Experimental verification of the SERS electromagnetic model beyond the E4 approximation: polarization effects, *J. Phys. Chem. C Lett.* 112 (2008) 8117–8121, <http://dx.doi.org/10.1021/jp802219c>.
- [28] M. Fan, G.F.S. Andrade, A.G. Brolo, A review on the fabrication of substrates for surface enhanced Raman spectroscopy and their applications in analytical chemistry, *Anal. Chim. Acta* 693 (2011) 7–25, <http://dx.doi.org/10.1016/j.aca.2011.03.002>.
- [29] S. Hong, X. Li, Optimal size of gold nanoparticles for surface-enhanced Raman spectroscopy under different conditions, *J. Nanomater.* (2013) 1–9, <http://dx.doi.org/10.1155/2013/790323>.
- [30] M. Moskovits, Surface-enhanced Raman spectroscopy: a brief retrospective, *J. Raman Spectrosc.* 36 (2005) 485–496, <http://dx.doi.org/10.1002/jrs.1362>.
- [31] K.G. Stamplecoskie, J.C. Scaiano, V.S. Tiwari, H. Anis, Optimal size of silver nanoparticles for surface-enhanced Raman spectroscopy, *J. Phys. Chem. C* 115 (2011) 1403–1409, <http://dx.doi.org/10.1021/jp106666t>.
- [32] P.N. Njoki, I.-S. Lim, D. Mott, et al., Size correlation of optical and spectroscopic properties for gold nanoparticles, *J. Phys. Chem. C* 111 (2007) 14664–14669, <http://dx.doi.org/10.1021/jp074902z>.
- [33] S.S. Masango, R.A. Hackler, N. Large, A.I. Henry, M.O. McAnally, G.C. Schatz, P.C. Stair, R.P. Van Duyne, High-resolution distance dependence study of surface-enhanced Raman scattering enabled by atomic layer deposition, *Nano Lett.* 16 (2016) 4251–4259, <http://dx.doi.org/10.1021/acs.nanolett.6b01276>.
- [34] V.T.N. Linh, J. Moon, C.W. Mun, V. Devaraj, J.-W. Oh, S.-Gy. Park, D.-H. Kim, J. Choo, Y.-I. Lee, H.S. Jung, A facile low-cost paper-based SERS substrate for label-free molecular detection, *Sens. Actuators B Chem.* 291 (2019) 369–377, <http://dx.doi.org/10.1016/j.snb.2019.04.077>.
- [35] A. Bonyár, I. Csarnovics, M. Veres, L. Himics, A. Csik, J. Kámán, B. Balázs, S. Kökényesi, Investigation of the performance of thermally generated gold nanoislands for LSPR and SERS applications, *Sens. Actuators B Chem.* 255 (2018) 433–439, <http://dx.doi.org/10.1016/j.snb.2017.08.063>.
- [36] Y. Huang, Q. Zhou, M. Hou, L. Ma, Z. Zhang, Nanogap effects on near- and far-field plasmonic behaviors of metallic nanoparticle dimers, *Phys. Chem. Chem. Phys.* 17 (2015) 29293–29298, <http://dx.doi.org/10.1039/c5cp04460j>.
- [37] Z. Skeete, H.-W. Cheng, Q.M. Ngo, Ch. Salazar, W. Sun, J. Luo, Ch.-J. Zhong, Squeezed interparticle properties for plasmonic coupling and SERS characteristics of duplex DNA conjugated/linked gold nanoparticles of homo/hetero-sizes, *Nanotechnology* 27 (2016) 325706, <http://dx.doi.org/10.1088/0957-4484/27/32/325706>.
- [38] H. Xu, E.J. Bjerneld, J. Aizpurua, P. Apell, L. Gunnarsson, S. Petronis, B. Kasemo, Ch. Larsson, F. Hook, M. Kall, Interparticle coupling effects in surface-enhanced Raman scattering, *Proc. SPIE* 4258, Nanoparticles and Nanostructured Surfaces: Novel Reporters With Biological Applications, 4258, 2001, pp. 35–42, <http://dx.doi.org/10.1117/12.430771>.
- [39] Z. Zhu, T. Zhu, Zh. Liu, Raman scattering enhancement contributed from individual gold nanoparticles and interparticle coupling, *Nanotechnology* 15 (2004) 357–364, <http://dx.doi.org/10.1088/0957-4484/15/3/022>.
- [40] K. Nehra, S.K. Pandian, M.S.S. Bharati, V.R. Soma, Enhanced catalytic and SERS performance of shape/size controlled anisotropic gold nanostructures, *New J. Chem.* 43 (2019) 3835–3847, <http://dx.doi.org/10.1039/c8nj06206d>.
- [41] H. Yockell-Lelièvre, F. Lussier, J.-F. Masson, Influence of the particle shape and density of self-assembled gold nanoparticle sensors on LSPR and SERS, *J. Phys. Chem. C* 119 (2015) 28577–28585, <http://dx.doi.org/10.1021/acs.jpcc.5b09570>.
- [42] Ch.J. Orendorff, A. Gole, T.K. Sau, C.J. Murphy, Surface-enhanced Raman spectroscopy of self-assembled monolayers: sandwich architecture and nanoparticle shape dependence, *Anal. Chem.* 77 (2005) 3261–3266, <http://dx.doi.org/10.1021/ac048176x>.
- [43] NanoComposix, Tools, NanoComposix, 2014 (accessed 30 Jan 2020 <http://nanocomposix.com/pages/tools>).
- [44] M. Quinten, *Optical Properties of Nanoparticle Systems: Mie and Beyond*, Wiley-VCH, Weinheim, Germany, 2011.
- [45] Y.-H. Kwon, R. Ossig, F. Hubenthal, H.-D. Kronfeldt, Influence of surface plasmon resonance wavelength on SERS activity of naturally grown silver nanoparticle ensemble, *J. Raman Spectrosc.* 43 (2012) 1385–1391, <http://dx.doi.org/10.1002/jrs.4093>.
- [46] B. Sharma, R.R. Frontiera, A.-I. Henry, E. Ringe, R.P. Van Duyne, SERS: materials, applications, and the future, *Mater. Today* 15 (2012) 16–25, [http://dx.doi.org/10.1016/S1369-7021\(12\)70017-2](http://dx.doi.org/10.1016/S1369-7021(12)70017-2).
- [47] R. Pilot, R. Signorini, C. Durante, L. Orian, M. Bhamidipati, L. Fabris, A review on surface-enhanced Raman scattering, *Biosensors* 9 (2019) 57, <http://dx.doi.org/10.3390/bios9020057>.
- [48] Y. Flegler, Y. Mastai, M. Rosenbluh, D.H. Dressler, Surface enhanced Raman spectroscopy of aromatic compounds on silver nanoclusters, *Surf. Sci.* 603 (2009) 788–793, <http://dx.doi.org/10.1016/j.susc.2009.01.020>.
- [49] Benzophenone datasheet in the NIST Chemistry WebBook, <https://webbook.nist.gov/cgi/cbook.cgi?ID=C119619&Mask=400#UV-Vis-Spec>.

Biographies

Petra Pál is a 1st year Ph.D. student at the Department of Experimental Physics, Faculty of Science and Technology, University of Debrecen. She has an M.Sc. degree in material science. She has 3 years of experience in Raman spectroscopy and Surface-enhanced Raman Scattering. She did her master thesis in this field and now continue the work during her Ph.D. studies.

Attila Bonyár is an associate professor at the Department of Electronics Technology at Budapest University of Technology and Economics. He has two M.Sc. degrees in electrical engineering and biomedical engineering and a Ph.D. in electrical engineering. He has 14 years of experience in the development of optical and electrochemical, affinity-type biosensors, utilizing low-dimensional nanomaterials, plasmonics, and nanometrology (AFM).

Miklós Veres is the head of the Department of Applied and Nonlinear Optics at the Institute for Solid State Physics and Optics, Wigner Research Centre for Physics. He has an M.Sc. degree in physics and a Ph.D. in physics in the field of investigation of carbon materials with Raman spectroscopy. He has 20 years of experience in Raman Spectroscopy, developing the SRS technique. He is leading a project based on nanostructures and applied spectroscopy.

László Himics is a research fellow at the Department of Applied and Nonlinear Optics at Institute for Solid State Physics and Optics, Wigner Research Centre for Physics. He has an M.Sc. degree in physics and a Ph.D. in physics in the field of investigation of diamond materials with Raman spectroscopy. He has 10 years of experience in Raman spectroscopy.

László Balázs is a physicist at the University of Debrecen. He has an M.Sc. degree in material science in the field of creation of metallic nanoparticles, investigating their parameters and their Localized Surface Plasmon Resonance characteristics. He did his master thesis in this field and now continue the co-operation with our group.

Laura Juhász is a 4th year Ph.D. student at the Department of Solid State Physics, Faculty of Science and Technology University of Debrecen. She has an M.Sc. degree

in physics. She is working in the field of creation and investigation of metallic-plasmonic structures and their properties. She has 4 years of experience in the field of Scanning Electron Microscope.

Istvan Csarnovics is an assistant professor at the Department of Experimental Physics, Faculty of Science and Technology, University of Debrecen. He has an M.Sc. in physics and a Ph.D. in physics in the field of photosensitive, inorganic materials, and investigation of the stimulation of photo-induced effects by the plasmon field of gold nanoparticles. He has 12 years of experience in the field of atomic force microscopy, creation and investigation of metallic nanoparticles, few years experience in the field of plasmonic sensing devices, Raman spectroscopy, and Surface-enhanced Raman scattering effect.